Chinese Journal of Chemistry, **2004**, *22*, 354—359 **Article**

Synthesis, Characterization and Two-Photon Absorption Properties of a Novel Pyridinium Salt

HAO, Fu-Ying[a,b](郝扶影) SHI, Peng-Fei[a](施鹏飞) LIU, Hui-Jun[a](刘会军)
WU, Jie-Ying[a](吴杰颖) YANG, Jia-Xiang[a](杨家祥) TIAN, Yu-Peng[*,a,c,d](田玉鹏)
ZHOU, Guang-Yong[d](周广勇) JIANG, Min-Hu[a,d](蒋民华)
FUN, Hoong Kun[e] SUCHADA, Chantrapromma[e]

[a] *Department of Chemistry, Anhui University, Hefei, Anhui 230039, China*
[b] *Department of Chemistry, Fuyang Normal School, Fuyang, Anhui 236032, China*
[c] *State Key Laboratory of Coordination Chemistry, Nanjing University, Nanjing, Jiangsu 210093, China*
[d] *State Key Laboratory of Crystal Materials, Shandong University, Jinan, Shandong 250100, China*
[e] *X-ray Crystallography Laboratory, School of Physics, Universiti Sains Malaysia, 11800 USM, Penang, Malaysia*

A novel pyridinium salt, 2,4-bis[*p*-(*N*,*N*-dimethylamino)styryl]-*N*-methyl pyridinium iodide (**BMSPI**) was synthesized and characterized by TG, ^{1}H NMR spectroscopy and elemental analysis, and the reaction process was studied by using ES-MS. When **BMSPI** was pumped by a pulsed 1064 nm, 50 ps laser beam, it manifests highly efficient TPA (Two-Photon Absorption) and up-conversion superradiance. The up-conversion efficiency was 6.0% at the pump energy of 4—6 mJ and the lifetime of two-photon fluorescence was measured as 59 ps.

Keywords pyridinium salt, two-photon induced fluorescence, reaction mechanism

Introduction

Materials with a large Two-Photon Absorption (TPA) cross section have been gained considerable attention in recent years owing to its applications in various fields, including optical data storage, lithographic micro-fabrication, laser device fabrication and photodynamic therapy.[1-5] Among them two-photon-induced fluorescence has received the wide popularity in the biological community and given rise to the development of two-photon laser scanning fluorescence microscopy. The molecule excitation by the simultaneous absorption of two photons, however, presents several advantages including a capacity for a highly confined excitation and intrinsic three-dimension resolution, and the possibility of imaging at an increased penetration depth in tissue, with reduced photo-damage and background fluorescence. These potential applications inevitably stimulated research on design, synthesis and characterization of new molecules with great TPA abilities. One of the largest classes of organics with large second-order polarizabilities consists of donor-acceptor (abbreviate as D, A, respectively) substituted stilbene. Among them, the DAMS$^+$ [4-{2-(4-dimethylaminophenyl)ethenyl}-1-methyl pyridinium cation] has been reported to exhibit one of the largest known frequency-doubling capacities.[6-8] But in the experiments, faint TPA was observed in DAMS$^+$I$^-$. In previous work of our research group, chromophores with different counterions and different side chains, both those changes resulted in highly efficient TPA properties have been synthesized.[9-17] And then a D-π-A-π-D type (or Λ shape) [D=donor, π=conjugation system, A=acceptor] pyridinium salt (BMSPI) was synthesized. It should be pointed out that this Λ shape molecule also showed good TPA ability as compared with DAMS$^+$I$^-$, a linear shape molecule with similar structure. In this paper, the intensive up-conversion superradiance and the TPA induced fluorescence of the title compound is reported.

Experimental

Materials and measurements

IR spectra were recorded on a Nicolet NEXUS 870 spectrometer with samples prepared a KBr pellets. The UV-visible spectrum was measured on a Hitachi 340 spectrometer using quartz curettes of 1-cm path length. Elemental analysis data were obtained using a Perkin-Elmer 240B elemental analyzer. ^{1}H NMR spectra were obtained on a Bruker Advanced/DMX 500 NMR spectrometer in DMSO-d_6 solution (TMS as internal standard in ^{1}H NMR). Thermal analyses were performed on a Perkin Elmer TGS-2 thermogravimetric

* E-mail: yptian@mars.ahu.edu.cn; Fax: 86-551-5107304
Received February 26, 2003; revised August 22, 2003; accepted December 13, 2003.
Project supported by the Major State Basic Research Development Program of China (No. G1998061402), the National Natural Science Foundation of China (Nos. 50272001, 20071001), the Natural Science Foundation of Anhui Province (No. 03044701) and the Malaysian Government and University Sains Malaysia for research grant K&D (No. 305/PFIZIK/610961).

analyzer. Electrospray mass spectrum (ES-MS) was recorded on a Finnigan LCQ mass spectrograph, and the concentration of the samples was about 1.0 mmol/mL. The diluted solution was electrosprayed at a flow rate of 5×10^{-6} L/min with a needle voltage of 4.5 kV. The mobile phase was an aqueous solution of methanol (*V*∶*V*, 1∶1). The samples were run in the positive-ion mode. Single–photon fluorescence spectrum was measured using a spectrofluophotometer (Perkin-Elmer LS55B). The two-photon fluorescence spectra were recorded using a passively mode-locked Nd∶YAG laser (Continuum, PY61C-10) as pump source, and a single-scan streak camera (Hamamatsu Model C5680, 2 ps resolution) together with a polychromator as a recorder. The pulse duration of the Nd∶YAG laser is 50 ps. The pump source was focused into the sample solution in a 1-cm glass cell by a convex lens (its focus is 15 cm). In the measurement of the fluorescence, the position of the glass cell was changed back and forward in the direction of the pump source until no superradiance could be observed. The fluorescence was collected into the slit of the streak camera by two short-focal-length convex lenses.

The crystal data for the complex were collected on a Siemens SMART CCD area detector diffractometer equipped with Mo Kα radiation using *ω*-scan mode. The unit cell parameters were determined using the program SMART (Siemens, 1996a). The three sets of data collected were reduced by using the program SAINT (Siemens, 1996b). The structure was solved with direct methods by using the program SHELXTL (Sheldrick, 1997). All the non-hydrogen atoms were located from the trial structure and then refined anisotropically with SHELXTL using full-matrix least-squares procedure. The hydrogen atoms were geometrically fixed at calculated positions attached to their parent atoms, and treated as riding atoms.

Preparations and characterization

The reaction steps are shown in Figure 1.

2,4-Dimethyl-*N*-methyl pyridinium iodide (DMPI)

2,4-Dimethyl pyridine (2.14 g, 0.02 mol) was dissolved in 10 mL of ethanol, then methyl iodide (4.32 g, 0.03 mol) was added dropwise into the solution. The mixture was heated to reflux at 80 ℃ for 40 min to give white microcrystals 4.23 g, yield 85%. ^{1}H NMR (DMSO-d_6, 500 MHz) δ: 2.54 (s, 3H), 2.71 (s, 3H), 4.15 (s, 3H), 7.71, 7.78 (d, J=6.13 Hz, 1H), 7.89 (s, 1H), 8.8 (d, J=6.4 Hz, 1H). Anal. calcd for $C_8H_{12}NI$: C 38.55, H 4.85, N 5.62; found C 38.53, H 4.80, N 5.60.

2-Methyl-4-[*p*-(*N*,*N*-dimethylamino)styryl]-*N*-methyl pyridinium tetraphenylborate (MSPTB)

DMPI (4.98 g, 0.02 mol), 4-(*N*,*N*-dimethylamino)-benzaldehyde (3.0 g, 0.02 mol) and 50 mL of ethanol were added into a 100 mL-flask with a stirrer and a condenser. Then four drops of piperidine were added. The solution was heated to reflux for 6 h to form 2-methyl-4-[*p*-(*N*-methyl-*N*-methylamino)styryl]-*N*-methylpyridinium iodide (**MSPI**). Then the solution was added into a solution of sodium tetraphenylborate (0.02 mol) in 50 mL of ethanol with stirring and heating simultaneously. After being refluxed for 4 h, the solution was cooled to room temperature with stirring. Evaporating the red solution yielded shinning microcrystals. Recrystallizing from acetonitrile the product formed deep-red parallelepiped crystals, which could be used for X-ray analysis. **MSPI**: ^{1}H NMR (DMSO-d_6, 500 MHz) δ: 2.69 (s, 3H), 3.03 (s, 6H), 4.08 (s, 3H), 6.79 (d, J=7.86 Hz, 4H), 7.84, 7.87 (d, J=16 Hz, 2H), 7.90 (s, 1H), 8.00 (d, J=6.1 Hz, 1H), 8.68 (d, J=6.69 Hz, 1H); IR (KBr) ν: 1375 (CH_3), 980 (RCH=CHR) cm^{-1}. Anal. calcd for $C_{41}H_{41}BN_2$: C 86.00, H 7.22, N 4.89, found C85.79, H 7.11, N 4.95.

2,4-Bis[*p*-(*N*,*N*-dimethylamino)styryl]-*N*-methyl pyridinium iodide (BMSPI)

DMPI (4.98 g, 0.02 mol), 4-(*N*,*N*-dimethylamino)-benzaldehyde (5.97 g, 0.04 mol) and 50 mL of ethanol were added into a 100 mL-flask equipped with a stirrer and a condenser. Then four drops of piperidine were added. The solution was heated to reflux for three days to form **BMSPI,** which was purified by column chroma-

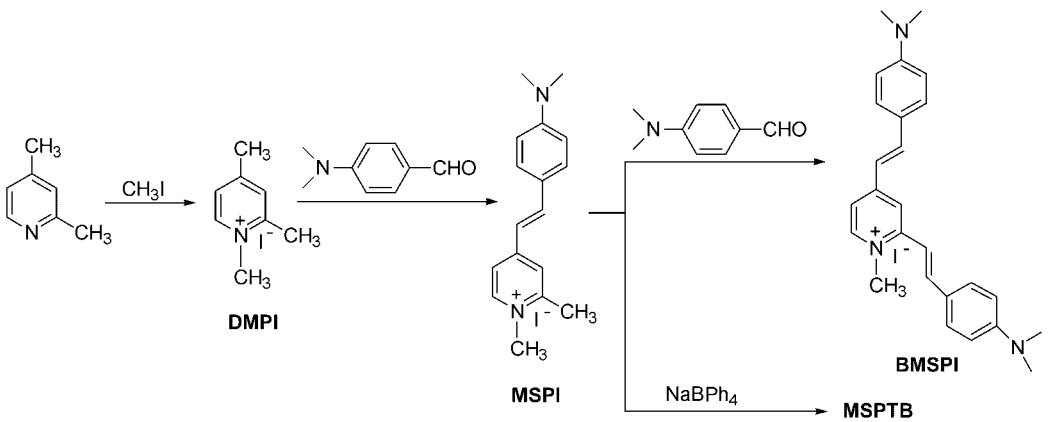

Figure 1 Preparative steps of BMSPI.

tography (Al_2O_3, CH_2Cl_2 : C_2H_5OH=5 : 1). ^1H NMR (DMSO-d_6, 500 MHz) δ: 3.03 (d, J=8.15 Hz, 12H), 4.15 (s, 3H), 6.79 (d, J=7.84 Hz, 4H), 7.14 (d, J=15.71 Hz, 2H), 7.56 (d, J=8.75 Hz, 2H), 7.68 (d, J=8.75 Hz, 2H), 7.76 (d, J=5.88 Hz, 1H), 7.84, 7.90 (d, J=13 Hz, 2H), 8.34 (s, 1H), 8.52 (d, J=6 Hz, 1H); IR (KBr) ν: 1368 (CH_3), 970 (RCH=CHR) cm^{-1}. Anal. calcd for $C_{26}H_{30}N_3I$: C 61.01, H 5.86, N 8.21; found C 61.03, H 5.89, N 8.01.

Results and discussion

Reaction steps of BMSPI

The molecular shape of **BMSPI** was designed to be Λ, and it required one molecule of **DMPI** to react with two molecules of 4-(*N*,*N*-dimethylamino)benzaldehyde. When the mixture of **DMPI** and aldehyde was heated to reflux for 6 h, only **MSPI** was obtained. By changing the counterion from I^- to tetraphenylborate, easily crystallized **MSPTB** could be obtained for X-ray structure determination, but as the reaction time was extended to 20 h, a mixture of **MSPI** and **BMSPI** was gotten. The relative new technique of electrospray mass spectrometry (ES-MS) allows preexisting ions in solution to be transferred very gently into the gas phase with minimal fragmentation.[18] It was used to study the reaction steps. From Figure 2, one can see two the peaks located at 253.5 and 384.5, respectively. The first peak represents the positive-ion of **MSPI**, the latter indicates that **BMSPI** had been produced already. Refluxing the reaction system for three days only yielded **BMSPI** as shown in Figure 3. So in this reaction, **BMSPI** was not produced by one molecule of **DMPI** reacting with two molecule of aldehyde immediately. In fact, one molecule of **DMPI** first reacted with one molecule of aldehyde, formed 2-methyl-4-[*p*-(*N*,*N*-dimethylamino)-styryl]-*N*-methylpyridinium iodide due to the stereo effect. As the reaction was going on, 2-methyl-4-[*p*-(*N*,*N*-dimethylamino)styryl]-*N*-methylpyridinium reacted with another aldehyde to form **BMSPI**, Λ shape molecule. So the reaction time is crucial to the target Molecule.

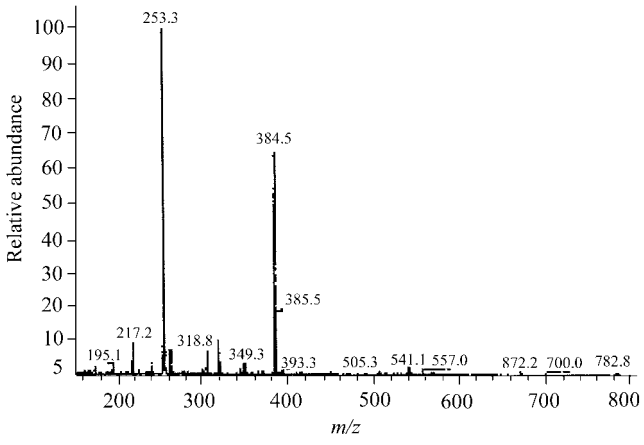

Figure 2 ES-MS of the solution in methanol (when reaction time was about 20 h in step two).

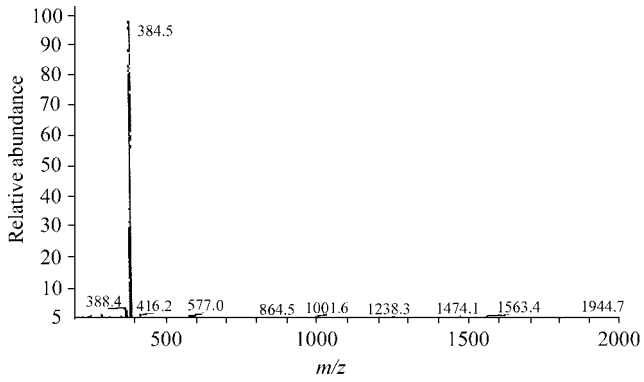

Figure 3 ES-MS of **BMSPI** in methanol solution.

Structure features of MSPTB and BMSPI

The crystal data and details of the structure determination for **MSPTB** are shown in Table 1. The selected bond lengths and the angles are listed in Table 2. The molecule structure is shown in Figure 4.

Table 1 Crystal data, diffraction data and refinement data of **MSPTB**

Compound	**MSPTB**
Empirical formula	$C_{41}H_{41}BN_2$
Formula weight	572.57
Color	Red
Crystal system, space group	Monoclinic, $P2_1/c$
Temperature/K	293(2)
Wavelength λ/nm	0.071073
a/nm	1.76291(1)
b/nm	1.13270(3)
c/nm	1.73485(4)
β/(°)	112.428(1)
Cell volume/nm^3	3.2022(11)
Z	4
Reflections collected/unique	21574/7770
	[R(int=0.1870]
Final R indices [$I>2\sigma(I)$]	R_1=0.0861, wR_2=0.1838
Extinction coefficient	0.0109(14)
Goodness-of-fit on F^2	0.828

From Figure 4, it is easy to find that the molecule is of *trans*-stilben structure. The pyridyl ring makes a dihedral angel of 15° to the phenyl ring. The maximum deviation for non-H atoms from the mean planes of the pyridyl and phenyl rings is 5.3×10^{-4} nm and 3.9×10^{-4} nm, respectively. The anion takes a slightly distorted tetrahedral geometry. The bond lengths of the pyridine ring and the phenyl ring are all of aromatic character. The bond lengths of C(6)—C(9), C(9)—C(10), C(10)—C(11) are 0.14567, 0.13294 and 0.14558 nm, respectively. These bridge bond lengths are even and

Table 2 Selected bond length (nm) and bond angels (°) of **MSPTB**

N(1)—C(3)	0.1386(7)	C(6)—C(7)	0.1359(10)
N(1)—C(1)	0.1446(7)	C(6)—C(9)	0.14567(10)
N(1)—C(2)	0.1459(7)	C(7)—C(8)	0.1378(9)
N(2)—C(14)	0.1366(7)	C(9)—C(10)	0.13294(10)
N(2)—C(13)	0.1365(6)	C(10)—C(11)	0.14558(10)
N(2)—C(17)	0.1490(6)	C(11)—C(12)	0.1348(8)
B(1)—C(24)	0.1652(7)	C(11)—C(15)	0.1334(8)
C(3)—C(4)	0.1405(7)	C(12)—C(13)	0.1360(7)
C(3)—C(8)	0.1403(8)	C(13)—C(16)	0.1470(7)
C(4)—C(5)	0.1367(8)	C(14)—C(15)	0.1340(8)
C(3)-N(1)-C(1)	121.4(5)	C(9)-C(10)-C(11)	129.7(8)
C(3)-N(1)-C(2)	119.5(5)	C(15)-C(11)-C(12)	120.3(6)
C(1)-N(1)-C(2)	117.9(5)	C(15)-C(11)-C(10)	107.6(7)
C(13)-N(2)-C(14)	119.5(5)	C(12)-C(11)-C(10)	132.0(8)
C(13)-N(2)-C(17)	122.0(5)	C(11)-C(12)-C(13)	122.3(6)
C(14)-N(2)-C(17)	118.5(6)	C(12)-C(13)-N(2)	117.2(5)
N(1)-C(3)-C(8)	122.2(6)	C(12)-C(13)-C(16)	125.3(6)
N(1)-C(3)-C(4)	120.5(6)	N(2)-C(13)-C(16)	117.5(5)
C(8)-C(3)-C(4)	117.3(6)	C(15)-C(14)-N(2)	121.9(6)
C(5)-C(4)-C(3)	119.6(6)	C(11)-C(15)-C(14)	118.8(6)
C(6)-C(5)-C(4)	123.9(7)	C(36)-B(1)-C(18)	107.5(4)
C(7)-C(6)-C(5)	116.2(7)	C(36)-B(1)-C(24)	108.3(4)
C(7)-C(6)-C(9)	136.1(10)	C(18)-B(1)-C(24)	111.2(4)
C(5)-C(6)-C(9)	107.3(9)	C(36)-B(1)-C(30)	109.6(4)
C(6)-C(7)-C(8)	123.5(7)	C(18)-B(1)-C(30)	110.7(3)
C(7)-C(8)-C(3)	119.6(6)	C(24)-B(1)-C(30)	109.4(4)

between typical single and double-bond length, indicating that **MSPTBs** are highly conjugated. The conjugated geometric configuration reveals that the cation has a highly delocalized π-electron system, which is a necessary condition for nonlinear optical response.

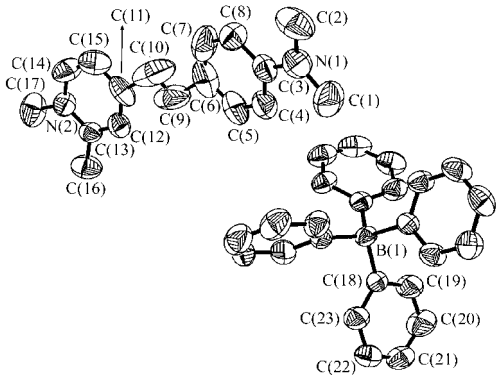

Figure 4 Molecular structure of **MSPTB**.

On the other hand, the *trans*-stilbene structure for **MSPTB** is also proved by its ^{1}H NMR spectral data [δ: 7.84, 7.87 (d, J=16 Hz, 2H)]. The further product, the title compound (**BMSPI**), posses a *trans*-stilbene derivation [δ: 7.09, 7.19 (d, J=15.71 Hz, 2H); 7.84, 7.90 (d, J=13.00 Hz, 2H)], but Λ shape. It has a larger delocalized π-electron system as compared with **MSPTB**, which may be the origin of TPA response.

TGA analysis of BMSPI

The TGA curve showed **BMSPI** had good thermostability. It would not lose weight until the temperature was up to 267 ℃. There was an 8.33% weight loss in the heating process from 266.7 ℃ to 282 ℃. It was proved to be a loss of a dimethylamino, and from 341.7 ℃ to 387.9 ℃ there was 35.07% loss of its weight, indicating that it lost iodide, another dimethylamino and the methyl bonded to the atom N of pyridine.

Linear absorption spectrum of BMSPI

Ethanol was chosen as the solvent for recording the spectra because of its excellent UV transparency. There are two absorption peaks located at 475 nm (with the corresponding mole absorption coefficient lg ε=3.92) and 544 nm (lg ε=4.77). There is no reasonable linear absorption in the spectral range from 600 nm to 1500 nm. From the linear absorption spectrum, one can image that TPA process might be expected in the wavelength range of 800—1200 nm. So the 1064 nm-pulsed laser was used as the pump source.[9,17,19]

Single and two-photon excited fluorescence of BMSPI

Figure 5 shows the single (a) and two-photon (b) fluorescence spectra of **BMSPI** solution in methanol. The peak position with a half highness is 617.6 nm with 52.4 nm (for single-photon fluorescence) and 623.5 nm with 52.7 nm (for two-photon fluorescence), respectively. From the figure, it can be seen that single and two-photon excited emissions come from the same energy level, but there is about 6 nm red shift for the peak position of TPA fluorescence (623.5 nm) compared with that of single-photon absorption fluorescence. This is due to the re-absorption effect of **BMSPI** solution at high concentration. The higher the concentration is, the more the re-absorption, and then the larger the red shift of the peak.

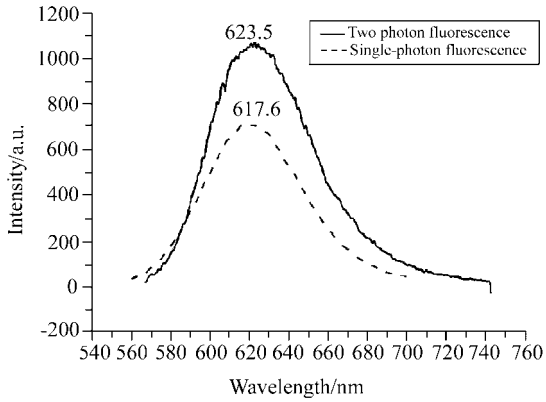

Figure 5 Single-photon and two-photon (of 1064 nm from mode-locked Nd∶YAG laser) excited fluorescence spectra of **BMSPI**.

Two-photon up-conversion superradiance and up-conversion efficiency of BMSPI

When a 1 cm-path **BMSPI** solution in DMF at 0.01 mol/L concentration was pumped by focused (its focus is 15 cm) picosecond 1064 nm laser beam, intense TPA fluorescence and superradiance can be observed, as shown in Figure 6, which shows the narrow intensive superradiance, and the peak position was at 625.3 nm with the bandwidth of 15.38 nm. It is obvious that the superradiance spectral width is much narrower than the fluorescence spectral width even without using any intracavity dispersion elements.

The up-conversion superradiance efficiency was measured by a two-channel energy meter (EPM-2000), and the pump energy transmitted into the sample was filtered by an IR-cut filter. Two Glan-Taylor polarizers were used to change the pump energy continuously. Figure 7 shows that the efficiency increased as the pump energy enlarged. The maximum of the efficiency could be as high as 6.2% when the input energy got to 4 mJ. However, in spite of the increased energies, the efficiency was stagnated by the saturation absorption of the pump energy.[19] It can be deduced that **BMSPI** has a potential application as an up-conversion laser dye, as efficient as the known one, ASPI (6.7% under the experiment setup, 0.05 mol/L solution in DMF, the output/input energy was 0.14 mJ/2.1 mJ).

The lifetime of two-photon-excited fluorescence was also measured by the streak camera equipped with a delay unit. A deconvolution procedure was applied based on a global optimization algorithm to fit the experimental results of the fluorescence decay curves. The influence of the pump laser was excluded by a computer program. In Figure 8 the scatter curve is the measured data and the solid curve is the fitted curve. The lifetime was measured to be 59 ps, almost as short as the pulse interval. It is indicated that the best pump source for this short lifetime laser dye should be a picosecond laser.

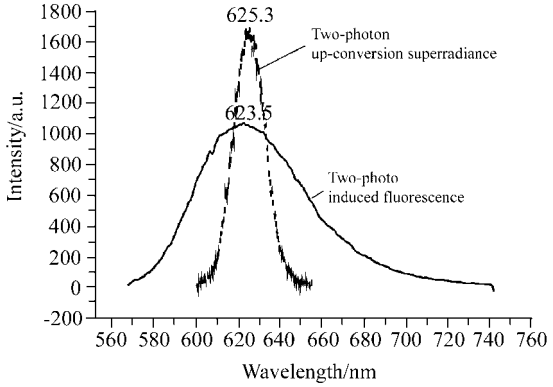

Figure 6 TPA fluorescence and up-conversion superradiance for **BMSPI**.

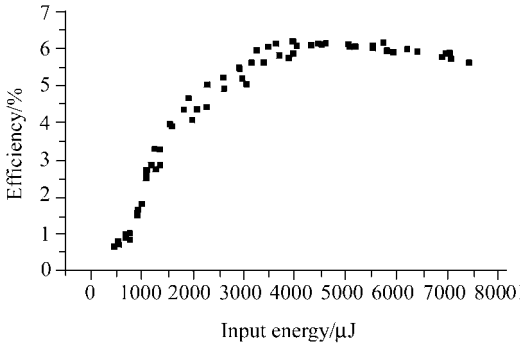

Figure 7 Up-conversion efficiencies of TPA superradiance at different pump energy at 1064 nm of **BMSPI** (The pump laser beam was produced by a mode-locked Nd∶YAG laser).

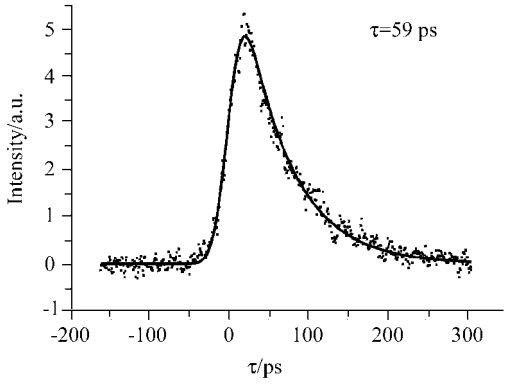

Figure 8 Lifetime of two-photon induced fluorescence of BMSPI solution in DMF (0.01 mol/L).

Conclusions

MSPI has a very weak TPA ability, which is similar to DAMS^{+}I^{-}. However, by changing the normal pyridinium salt with a D-π-A structure into a Λ shape (or D-π-A-π-D) molecule (**BMSPI**), it displays strong TPA excited fluorescence and up-conversion superadiance. So it could be deduced that changing the shape of a molecule is another way to get the compounds with strong TPA response.

References

1 Strickler, J. H.; Webb, W. W. *Opt. Lett.* **1991**, *16*, 780.
2 Compston, B. H.; Ananthavel, S. P.; Barlow, S.; Dyer, D. L.; Ehrlich, J. E.; Erskine, L. L.; Heikal, A. A.; Kuebler, S. M.; Sandy Lee, I. Y.; Mecord-Maughon, D.; Qin, J.; Rockel, H.; Rumi, M.; Wu, X. L.; Marder, S. R.; Pery, J. W. *Nature* **1999**, *398*, 51.
3 Zhao, C. F.; He, G. S.; Bhawalkar, J. D.; Park, C. K.; Prasad, P. N. *Chem. Mater*. **1995**, *7*, 1979.
4 He, G. S.; Yuan, L. X.; Cui, Y. P.; Li, M.; Prasad, P. N. *J. Appl. Phys*. **1997**, *81*, 2529.
5 He, G. S.; Signorini, R.; Prasad, P. N. *Appl. Opt*. **1998**, *37*, 5720.
6 Pascal, G.; Lacroix, R.C.; Keitaro, N.; Zyss, J.; Isabelle, L. *Science* **1994**, *263*, 658.
7 Marder, S. R.; Perry, J. W.; Schaefer, W. P. *Science* **1989**, *245*, 626.
8 Pascal, G. L.; Isabelle M. *Chem. Mater.* **2001**, *13*, 441.
9 Ren, Y.; Fang, Q.; Yu, W. T.; Lei, H.; Tian Y. P.; Jiang, M. H.; Yang, Q. Y.; Thomas, C. W. *J. Mater. Chem.* **2000**, *10*, 2025.
10 Tian, Y. P.; Yu, W. T.; Fang, Q.; Jiang, M. H.; Wang, H. Z. *Chin. J. Chem.* **2001**, *19*, 371.
11 Wang, X. M.; Wang, D.; Zhou, G. Y.; Yu, W. T.; Zhou, Y. F.; Fang, Q.; Jiang, M. H. *J. Mater. Chem.* **2001**, *11*, 1600.
12 Wang, D.; Wang, X.; Zhou, G. R.; Shao, Z. S.; Jiang, M. H. *Appl. Phys. B* **2001**, *73*, 227.
13 Zhou, G. Y.; Ren, Y.; Wang, D.; Wang, C.; Shao, Z. S.; Fang, Q.; Jiang, M. H. *Appl. Phys. B* **2001**, *72*, 937.
14 Tian, Y. P.; Yu, W. T.; Fang, Q.; Wu, J. Y.; Jiang, M. H.; Wang, H. Z.; Zhang, X. G. *Chem. Res. Chin. Univ.* **2002**, *18*, 211.
15 Zhou, G. Y.; Wang, X. M.; Wang, D.; Wang, C.; Zhao, X.; Shao, Z. S.; Jiang, M. H. *Opt. Laser Technol.* **2001**, *33*, 209.
16 Wang, X. M.; Wang, C.; Yu, W. T.; Zhou, Y. F.; Zhao, X.; Fang, Q.; Jiang, M. H. *Can. J. Chem.* **2001**, *79*, 171.
17 Lei, H.; Wang, H. Z.; Ren, T.; Fang, Q.; Zheng, X. G.; Wei, Z. C.; Xu, N. S.; Jiang, M. H. *Opt. Commun.* **2001**, *187*, 231.
18 Agostin, A.; Traeger, J. C. *Mass Spectrom. Rev.* **1995**, *14*, 79.
19 Wang, H. Z.; Lei, H.; Ren, Y.; Fang, Q.; Zheng, X. G.; Wei, Z. C.; Tian, Y. P.; Jiang, M. H. *Chem. Phys. Lett.* **2000**, *327*, 450.

(E0302269 SONG, J. P.)